DEVELOPMENT OF AN ADVANCED CONSTITUTIVE MODEL FOR SPOIL-STRUCTURE INTERACTION PROBLEMS

OPRACOWANIE ZAAWANSOWANEGO MODELU KONSTYTUTYWNEGO DLA ODDZIAŁYWAŃ ZWAŁOWISKO-KONSTRUKCJA BUDOWLANA

Nhat-Phi Doan, Anna Liakou, Thejesh Kumar Garala, Ge Cui, Naman Kantesaria, Koushik Halder, Charles M. Heron, Alec M. Marshall - Faculty of Engineering, University of Nottingham, United Kingdom

Revitalisation options for mine spoil heaps is an important issue to consider when planning for post-mining land use. One option is the installation of wind turbines on the spoil heaps, which provide a sustainable energy source. This option poses challenges for foundation design due to the nature of the spoil material, which is usually highly heterogeneous due to the way spoils are deposited, and can contain high proportions of high-plasticity cohesive soils (clay). This paper presents results obtained using an advanced constitutive model that was developed to simulate cohesive mine spoil behaviour and presents model results for the prediction of foundation response under both monotonic and cyclic loading. The model is a modified version of the original isotropic bounding surface plasticity model that additionally involves a damaged-based plastic modulus in order to realistically represent soil strength degradation induced by cyclic action. The model is used for the simulation of shallow foundations for onshore wind turbines on a cohesive clay with a heterogeneous (linearly increasing) undrained shear strength (random spatial variability is not considered). Two different loading scenarios of a shallow strip foundation are considered in the paper: a pure moment-vertical loading (M-V), and a moment-horizontal-vertical loading (M-H-V). The effect of the adopted spoil-foundation interface type is also considered: (1) a fully-bonded interface and (2) a tensionless interface. Results demonstrate that, though the vertical bearing capacity is only slightly affected by the interface properties, the moment capacity is shown to be strongly influenced by the predefined contact conditions. For the footing system under M-H-V loading, a dominant footing uplift mechanism is obtained for light structures and the opposite holds for heavily loaded structures, where significant settlement accumulation occurs during cyclic loading. Based on the analysis, the moment bearing capacity of the footing system decreases as the slenderness ratio and/or the vertical safety factor increase, and the opposite mechanism is obtained as the strength heterogeneity degree increases.

Keywords: *spoil, numerical modelling, constitutive model, rocking, cyclic loading*

Możliwości rewitalizacji zwałowisk są ważnym zagadnieniem przy planowaniu zagospodarowania terenów pogórniczych. Jedną z opcji jest instalacja na hałdach turbin wiatrowych, które stanowią zrównoważone źródło energii. Opcja ta stanowi wyzwanie dla projektowania fundamentów biorąc pod uwagę charakter materiału zwałowego, który ze względu na sposób deponowania jest zwykle wysoce niejednorodny i może zawierać dużo wysokoplastycznych gruntów spoistych (iłów). W artykule przedstawiono wyniki uzyskane przy użyciu zaawansowanego modelu konstytutywnego, który został opracowany w celu symulacji zachowania spoistego materiału zwałowego oraz zaprezentowano wyniki modelowania dla przewidywania reakcji fundamentu będącego zarówno pod obciążeniem monotonicznym jak i cyklicznym. Model jest zmodyfikowaną wersją oryginalnego izotropowego modelu plastyczności powierzchni granicznej, który dodatkowo zawiera moduł plastyczności oparty na zniszczeniu w celu realistycznego przedstawienia degradacji wytrzymałości gruntu wywołanej działaniem cyklicznym. Model jest wykorzystywany do symulacji płytkich fundamentów turbin wiatrowych na iłach spoistych o niejednorodnej (liniowo wzrastającej) wytrzymałości na ścinanie bez odpływu (nie uwzględniono losowej zmienności przestrzennej). W pracy rozpatrzono dwa różne scenariusze obciążenia płytkiej ławy fundamentowej: czyste obciążenia moment- pionowe (M-V) oraz obciążenia moment-poziome-pionowe (M-H-V). Rozważono również wpływ przyjętego rodzaju styku zwałowisko-fundament: (1) całkowicie związany oraz (2) beznaprężeniowy. Wyniki pokazują, że choć nośność pionowa tylko w niewielkim stopniu zależy od właściwości styku, to okazuje się, że nośność momentu jest silnie uzależniona od zdefiniowanych wcześniej warunków kontaktowych. Dla systemu stopy fundamentowej pod obciążeniem M-H-V, w przypadku lekkich konstrukcji uzyskuje się dominujący mechanizm unoszenia stopy, a w przypadku konstrukcji silnie obciążonych odwrotny, gdzie podczas cyklicznego obciążenia następuje znaczna akumulacja osiadań. Na podstawie przeprowadzonej analizy można stwierdzić, że nośność systemu stopy fundamentowej maleje wraz ze wzrostem współczynnika smukłości i/lub pionowego współczynnika bezpieczeństwa, a odwrotny mechanizm uzyskuje się wraz ze wzrostem stopnia niejednorodności wytrzymałości.

Słowa kluczowe: *zwałowisko, modelowanie numeryczne, model konstytutywny, przechylenie, obciążenie cykliczne*

Introduction

The long-term revitalisation of mining areas is an increasingly important issue being considered globally. Surface mining activities create large amounts of spoils or overburden mine wastes, which are typically dumped at a location located close to the mine site. Mine spoils generally have significant spatial variation of material types and properties (Masoudian et al. 2019a, Zevgolis et al. 2021), which creates challenges in terms of the use of the spoil material for engineering purposes. Revitalisation options for mine spoil heaps that are of particular interest are those that provide social and/or economic benefits, for example lake/forestry areas or installation of renewable energy infrastructure (photovoltaic cells or wind turbines). This paper focuses on the modelling of the response of cohesive spoil materials to monotonic and cyclic loading, with particular relevance to the development of wind turbines on mine spoil heaps.

This paper presents results obtained using an advanced constitutive model that was developed to simulate cohesive mine spoil behaviour with a heterogeneous (linearly increasing) undrained shear strength (random spatial variability is not considered) for the prediction of foundation response under both monotonic and cyclic loading. A bounding surface plasticity model (BSP) is proposed; the main difference of the bounding surface approach when compared to a classical elastoplasticity theory is the inclusion of a bounding surface rather than a yield surface, which functions as a lower/upper "bound" (Dafalias 1986). The application of a BSP model becomes essential if cyclic loading conditions are considered, as experimental evidence clearly demonstrates a hysteretic response and a progressive convergence of the stress-strain curve to a particular state after a certain number of cycles. In this study, a modified version of the original isotropic BSP model is adopted (Dafalias and Herrmann 1986), as it additionally involves a damage-based plastic modulus in order to realistically represent a soil strength degradation mechanism induced by a cyclic load action. The constitutive model is implemented in a UMAT subroutine in connection with the ABAQUS finite element (FE) software program. The FE model is used for the simulation of typical shallow foundations applicable to onshore wind turbines. Two shallow foundation loading scenarios are considered in the paper: a surface strip footing under pure moment-vertical loading (M-V), and a surface strip footing under moment-horizontal-vertical loading (M-H-V).

Constitutive model parameters and calibration

Several alternative versions of a BSP model are available in the literature (Kaliakin and Nieto-Leal 2013; Shi et al. 2019; Seidalinov and Taiebat 2014) which consider anisotropy, time--dependency, or strain degradation effects in a realistic manner. These models involve a large number of material parameters and, as a result, their application is prohibitive for practical purposes. To take advantage of the BSP model and further retain a simple formulation, an isotropic version of the (BSP) model is utilized, which additionally involves a damage factor for capturing soil strength degradation effects under a cyclic load action. Further details can be found in Dafalias and Herrmann (1986); Seidalinov and Taiebat (2014). A full description of the constitutive model is not possible in this paper; a summary of the input parameters is provided below.

In Tab.1, the model parameters that need to be calibrated based on element testing are summarized. Isotropic or one-dimensional consolidation test results are utilized to calculate the slopes of the normal compression line (NCL) λ and the recompression line (RL) κ in e– ln p' space (where e is void ratio and p' is mean effective stress). In addition the permeability k, and the initial void ratio e_N at p' = 1 kPa on the NCL are required.

The Poisson's ratio v can be evaluated by the graphs of the deviatoric stress q versus the axial strain ε_1 and the excess pore pressure u_e with respect to the axial strain ε_1, which are obtained from a monotonic consolidated-undrained triaxial test of a normally consolidated soil (Over-Consolidation Ratio OCR=1). If a constant shear modulus G is considered rather than a pressure-dependent formula, its value can be deduced by the initial slope of the graph of the deviatoric stress q versus the axial strain ε_1 that is derived by a consolidated-undrained (CU) triaxial test of a normally consolidated soil (OCR=1).

The slope M_c of the critical state line in p' - q space for triaxial compression is determined by calculating the ultimate values of p' and q for each element test (monotonic triaxial test), and subsequently drawing a straight line through the origin and the former ultimate values. Its value can be also directly derived by the effective friction angle of the soil; $M_c=(6\sin\phi')/(\sin\phi')$, where ϕ' is the soil critical state friction angle. To physically understand the effect of the slope M_c, it is important to mention that its increase implies a stronger/stiffer material response. The same calibration process is followed under triaxial extension such that the quantity γ_M is further determined.

Parameter R: a good estimate of the shape parameter R can be obtained by conducting a CU triaxial compression test of a normally consolidated sample (OCR = 1.0). Before shearing, the isotropic state is denoted by the stress point $(p'_0,0)$. During shearing, the critical state line at a mean normal effective stress of $p'=p'_f$ and deviatoric stress $q_f=Mc_{p'_f}$ are ultimately reached, and the parameter R can be accordingly evaluated by $R=\left(\frac{p'_0}{p'_f}\right)^{\frac{\lambda}{\lambda-\kappa}}$ as long as the parameters λ, κ and the mean efective stresses p'_0 and p'_f are known.

Projection centre parameter C: Undrained triaxial tests under different OCRs can be used for a first estimate of the projection centre parameter C, which will lie in the range $0\leq C<1$. If C=0, the projection centre coincides with the origin of the invariant stress space. Any increase in C leads to a decrease in initial pore pressure under undrained conditions (or increase of dilation under drained conditions). Furthermore, its magnitude does not affect the ultimate values of the deviatoric stress q, mean normal effective stress p', and pore pressure u. To enable a more accurate evaluation of the projection centre parameter C, both triaxial compression and extension tests would be necessary, while its calibration should also be combined with the simultaneous calibration of the hardening parameter h_c.

Hardening parameter h_c: under a monotonic triaxial compression test, the degree of inelastic hardening increases with an increase of the hardening parameter h_c. This further implies a stiffer material response as the plastic modulus K_p is also enhanced and a decrease in the excess pore pressure developed under undrained conditions. As explained above,

Tab.1. Material parameters of constitutive model and values for Drammen clay used in calibration analyses
Tab. 1. Parametry materiałowe modelu konstytutywnego i wartości dla ilu „Drammen" użyte w analizach kalibracyjnych

Parameters	Symbol	Value	
Slope of normal compression line in e– ln $p^{\wedge}{}'$ space	λ	0.26	
Slope of recompression line in e– ln $p^{\wedge}{}'$ space	K	0.035	
Slope of critical state line for triaxial compression	M_c	1.15	y_M=0.65
Poisson ratio	v	0.15	
Projection centre for triaxial compression	C	0	
Size of elastic nucleus for triaxial compression	s_c	1.55	y_s=0.85
Shape configuration parameter	R	2.4	
Hardening parameter for triaxial compression	h_c	370	y_h=0.65
Degradation parameter	α	0.1	
Unit weight (kN/m^3)	γ	17	
Void ratio at $p^{\wedge}{}'$ = 1kPa on NCL	e_N	2.4	
Permeability (m/s)	k	1x10^{-10}	

e = void ratio; γ_M,γ_s,γ_h: quantities related to triaxial extension when compared to associated values under triaxial compression.

its value is best calibrated in combination with the projection centre parameter C. The same procedure needs to be followed under triaxial extension such that the quantity γ_h is also determined.

Size of elastic nucleus for triaxial compression s_c: can be indirectly derived by CU triaxial compression tests; its value is closely related to the inelastic strains. Therefore, its calibration is also best combined with the aforementioned parameters. Nevertheless, its value is shown to be more important under cyclic loading. Therefore, cyclic triaxial tests are better used for its calibration combined with the associated quantity γ_s. In particular, the accumulated shear strain history deduced by a cyclic stress-controlled triaxial test or direct shear test can be used for the calibration of these parameters. Their evaluation is also combined by the calibration of the degradation parameter α.

Degradation parameter α: included in the expression of the hardening function and defines its softening under cyclic loading. Since its value is closely related to the shear strain history deduced by cyclic loading, cyclic stress-controlled triaxial tests and direct shear tests can be used for its evaluation. As explained above, its calibration is best combined with the calibration of the size of the elastic nucleus for triaxial compression s_c and the associated quantity γ_s.

Tab.2. Load notation
Tab. 2. Oznaczenia obciążenia

	Vertical	Horizontal	Moment
Load	V	Q	M
Ultimate Load	V_u	Q_u	M_u
Dimensionless Load	$\mathcal{V} = V/As_{uo}$	$\mathcal{Q}$	$\mathcal{M} = M/ABs_{uo}$
Normalized load wrt Ultimate Load	$v = V/V_u$	$q = Q/Q_u$	$m = M/M_u$
Displacement	w	δ	ϑ

The constitutive model parameters were calibrated using the data available in the literature for Drammen clay, a Norwegian marine clay with a plasticity index of I_p = 27%. Drammen clay was chosen for calibration of the constitutive model because extensive element testing has been performed by Andersen and his co-workers (Anderson et al. 1988; Anderson 2015; Thian and Lee 2014) which specifically involves oedometer tests, monotonic and cyclic simple shear tests and triaxial tests for distinct overconsolidation ratios OCRs, for various permanent and cyclic deviatoric levels, and a large number of cycles, N = 100. The calibrated material parameters are summarised in Tab.1. To enable the use of the constitutive soil model in connection with the ABAQUS software program, a UMAT user subroutine was developed.

Results - Monotonic and cyclic response of shallow foundations

A surface strip footing is considered, which rests on a heterogeneous clay deposit (i.e., gradient of strength k_h and shear strength profile s_u with depth z) and rigid bedrock underlies the clay. A linearly increasing undrained shear strength with depth is assumed that is given by s_u=s_{uo}+$k_h z$, where s_{uo} is the undrained shear strength at the foundation base level, while the soil strength heterogeneity degree κ_h can be described as κ_h=(k_h B)/s_{u0} (Vulpe et al., 2014).

Two interface properties are considered; (1) a fully-bonded contact, which does not allow separation and sliding of the foundation from the soil and (2) a tensionless interface that permits separation and further involves rough sliding conditions (Seidalinov and Taiebat, 2014). Even though the vertical bearing capacity is only slightly affected by the interaction properties,

the moment capacity is shown to be strongly influenced by the predefined contact conditions. The moment response under cyclic loading is also subsequently affected by the contact conditions. Sign conventions follow the recommendations of Butterfield et al. (1997) and the load and displacement notations are summarized in Tab.2.

Problem 1: footing response under pure moment-vertical action

A plane-strain finite-element mesh was adopted in order to model the surface strip footing of width *B*, which is described as a discrete rigid body with a reference point located at the centroid of the foundation, and the soil is represented by second-order reduced integration stress–pore fluid continuum elements. To eliminate any boundary effects on the foundation response, sufficient distance of the lateral and horizontal mesh boundaries from the strip footing were considered. In particular, a mesh half-width $L = 10B$ and depth $H = 10B$ was adopted.

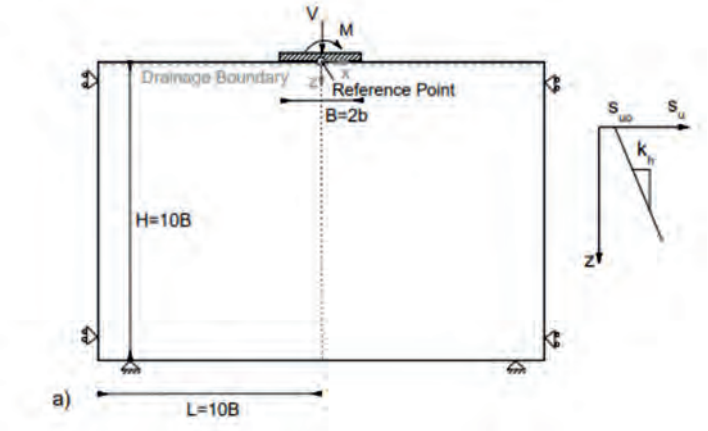

Fig. 1. FE model for Problem 1: footing response under a pure M-V action
Rys. 1. Model FE dla problemu 1: reakcja stopy pod wpływem czystego oddziaływania M-V

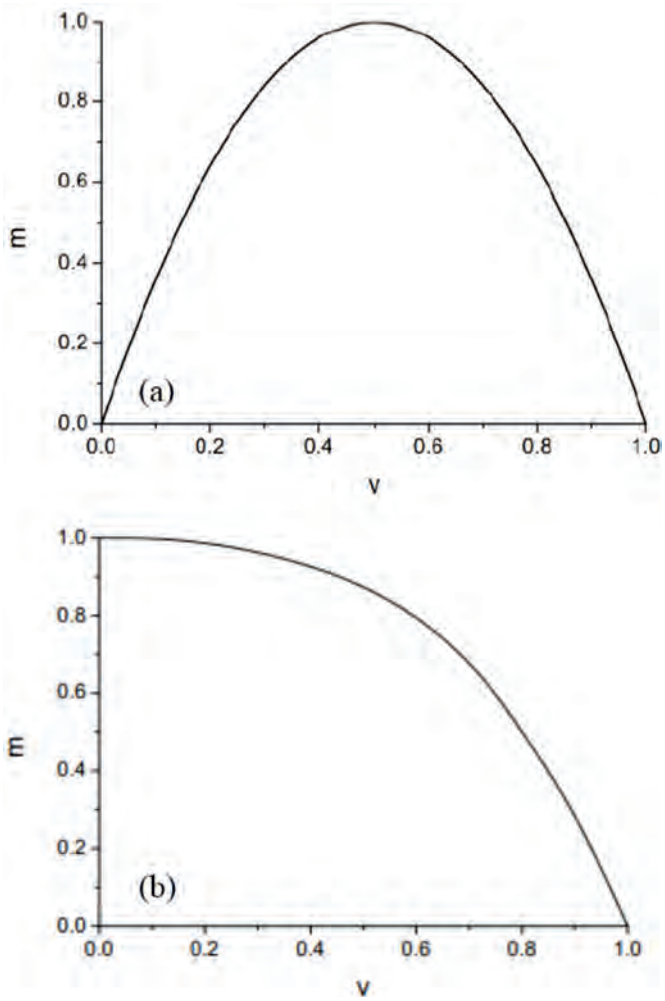

Fig. 2. m-v curves for (a) a tensionless interface and (b) a fully-bonded contact.
Rys. 2. Krzywe m-v dla (a) styku beznaprężeniowego i (b) całkowicie związanego.

Zero-horizontal and vertical displacement was assigned at the lower horizontal mesh boundary, while the lateral boundaries were constrained from horizontal displacement. The free surface was assigned at the upper soil surface, while the other mesh boundaries were assumed to be impermeable.

A quasi-static analysis was performed where a rotational displacement was applied at the footing centre under the action of a constant vertical load (M-V action). The resultant forces and displacements are accordingly measured at the reference point, as shown in Fig. 1.

Static Bearing Capacity

For a tensionless interface, the maximum moment capacity is obtained for a vertical safety factor $FS_v = v_u/v = 2$, while its value becomes zero when $v \rightarrow 0$ or $v \rightarrow 1$, as shown in Fig. 2a (Gazetas et al. 2013). If a fully-bonded contact is considered, a different failure envelope m-v is obtained when compared to the tensionless interface case. For a monotonic loading case, the ultimate moment capacity is maximum at a very high vertical safety factor, while its magnitude progressively decreases with increasing the vertical load, as shown in Fig. 2b).

Cyclic bearing capacity

The cyclic moment response and vertical displacement history with respect to the applied rotational displacement is shown in Fig. 3 and Fig. 4 for tensionless and fully-bonded interfaces. For a tensionless interface: a smoother response and moment hardening or softening depending on the vertical load level is obtained. In particular, a moment softening response is deduced and its variation rate decreases with the number of cycles (material nonlinearity). Furthermore, a substantial footing uplift is observed at the maximum rotation angle $\vartheta = |\vartheta_0|$ (geometric nonlinearity) that tends to decrease with the number of cycles along with a slight settlement accumulation at $\vartheta = 0$ (soil plasticity). For the fully-bonded interface: a very stiff response of moment *m* – rotation angle ϑ can be seen. The enclosed area of the moment-rotation angle is large (high damping ratio), and its shape remains almost unchanged during the cyclic loading. This fact is also confirmed by the soil reaction distribution along the footing interface that is not affected by the cyclic load action.

Problem 2: Slender-footing behaviour under combined moment-vertical-horizontal action

Identical geometric and boundary conditions from Problem 1 are considered for Problem 2, with the addition of an elevated mass *m*, which represents a thin rigid structure of a slenderness ratio $H=B$ (Fig. 5). The thin structure is represented as a discrete rigid body, similar to the strip footing. A pushover analysis is performed, which involves the application of a lateral displacement at the lumped mass. The resultant loads and displacements are computed at the

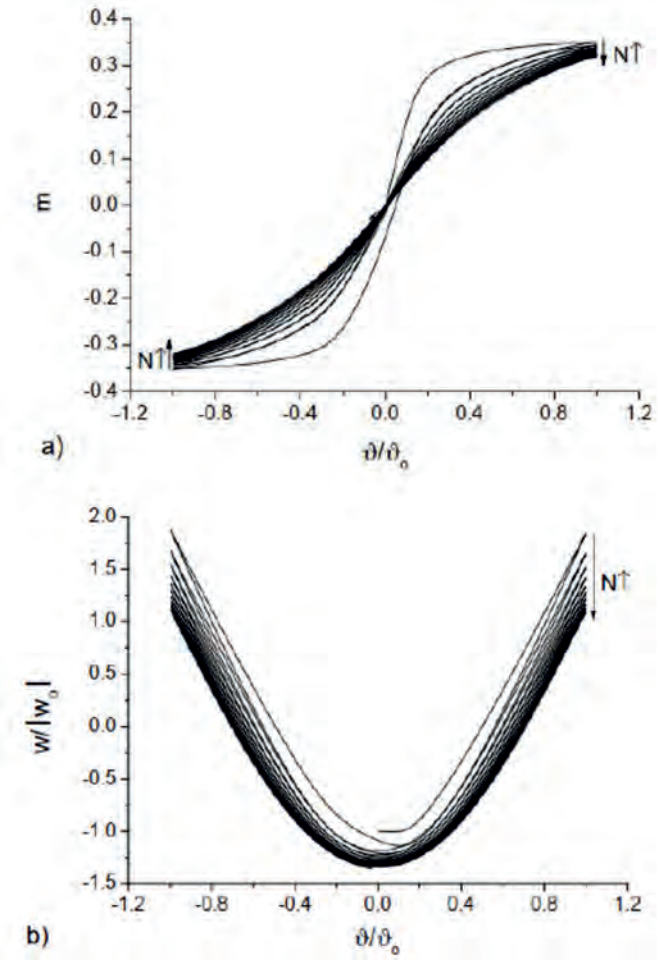

Fig. 3 a) Normalized moment and b) settlement with respect to normalized rotation angle for tensionless interface for ϑ_0 = 0.02rad, heterogeneity degree κ_h = 0.4, overconsolidation ratio OCR = 4, vertical safety factor FS_v = 10, N = 10 number of cycles and initial settlement w_o = -1.7mm.

Rys. 3 a) znormalizowany moment i b) osiadanie w odniesieniu do znormalizowanego kąta obrotu dla styku beznaprężeniowego dla ϑ_0 = 0.02rad, stopnia niejednorodności κ_h = 0.4, współczynnika prekonsolidacji OCR = 4, pionowego współczynnika bezpieczeństwa FS_v = 10, N = 10 liczby cykli i osiadania początkowego w_o = -1,7mm.

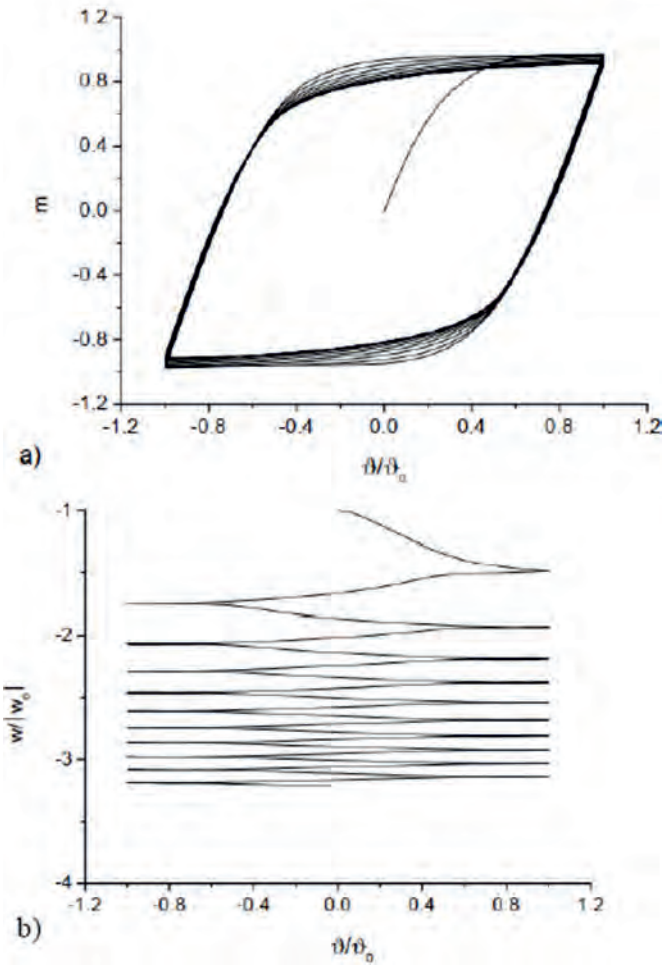

Fig. 4 a) Normalized moment and b) settlement with respect to normalized rotation angle for fully-bonded interface for ϑ_0 = 0.02rad, heterogeneity degree κ_h = 0.4, overconsolidation ratio OCR = 4, vertical safety factor FS_v = 10, and N = 10 number of cycles and initial settlement w_o = -1.7mm

Rys. 4 a) znormalizowany moment i b) osiadanie w odniesieniu do znormalizowanego kąta obrotu dla styku całkowicie związanego dla ϑ_0 = 0.02rad, stopnia niejednorodności κ_h = 0.4, współczynnika prekonsolidacji OCR = 4, pionowego współczynnika bezpieczeństwa FS_v = 10, oraz N = 10 liczby cykli i początkowego osiadania w_o -1,7mm

reference point, as before. Both small- and large-displacement analyses are performed in order to better evaluate the involved geometric nonlinearities that arise from the self-weight contribution on the resultant moment (*P-δ* effect). To account for nonlinear geometric effects (*P* - *δ*) in the finite element analysis stiffness matrix that are caused by large displacements, the "NLgeom" (Non-Linear geometry) option needs to be active in the step module of ABAQUS/Standard.

Monotonic and cyclic pushover analyses were performed, which provide important information regarding the thin rigid superstructure-foundation response. All numerical analyses assume a tensionless interface. Special attention is placed on the slenderness ratio effect and the evaluation of the *P* - *δ* effect.

Monotonic pushover analysis

A pushover method is a well-known technique in structural engineering for the analysis of tall slender structures resting on shallow foundations that are subjected to a monotonic or cyclic lateral displacement. The method is particularly useful for understanding and evaluating the *P* - *δ* effect. In the current study, a strip footing of width B = 2b supports an elevated mass, which represents a thin rigid structure of height $\vartheta\mathfrak{H}$ with a resulting slenderness ratio $\vartheta\mathfrak{H}/B$. A monotonically increasing lateral displacement is then applied at the elevated mass until toppling failure occurs (state of zero moment). The outcome of the analysis involves the history of the external moment at the reference point (RP) with respect to the applied lateral displacement. To enable the investigation of the *P-δ* effect, a large displacement analysis (L.D.A.) is performed (using the "NLgeom" option in ABAQUS), while its result is further compared with the outcome of a classical small displacement analysis (S.D.A.).

Fig. 6 illustrates the *P* - *δ* effect that is taken into account in a large displacement analysis is the reason behind the difference in the deduced *M* - *ϑ* responses, causing the reduced moment capacity and the softening behaviour when compared to the small-displacement analysis that ignores this effect. To be more specific, as the lateral displacement *δ* progressively increases, the moment component *P-δ* due to the self-weight contribution progressively increases, the magnitude of which becomes more pronounced as the vertical safety factor FS_v is reduced and/or the slenderness ratio increases.

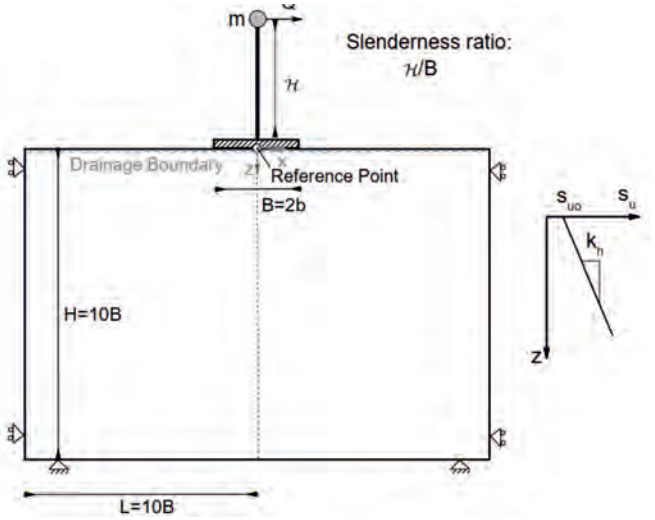

Fig. 5. FE model for Problem 2: slender-footing behaviour under combined M-V-Q action

Rys. 5. Model FE dla problemu 2: zachowanie się smukłej stopy fundamentowej pod połączonym oddziaływaniem M-V-Q

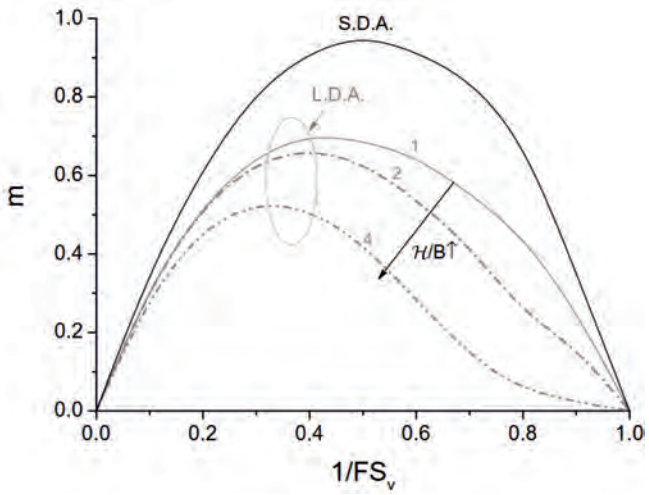

Fig. 6. The *P-δ* effect and slenderness ratio effect $\mathcal{H}/B$ = (1,2,4) on moment capacity m with respect to the inverse vertical safety factor 1/FSv, material properties OCR = 4 and κ_h = 0.4

Rys. 6. Efekt *P-δ* i efekt współczynnika smukłości $\mathcal{H}/B$ = (1,2,4) na nośność momentu m w odniesieniu do odwrotnego pionowego współczynnika bezpieczeństwa 1/FS$_v$, właściwości materiałowych OCR = 4 i κ_h = 0,4

A parametric analysis was performed for different vertical load levels, heterogeneity degrees, and slenderness ratio. Both S.D.A. and L.D.A. were conducted and results are shown in Fig. 7. From the graph, for an S.D.A., the moment capacity increases with the slenderness ratio, while the opposite holds for a L.D.A., independent of the heterogeneity degree. For a low heterogeneity degree κ_h = 0.4, the discrepancy between the S.D.A. results for different slenderness ratios $\mathcal{H}/B$ = (2,4,8) is less significant when compared to the higher heterogeneity degree level κ_h = 4. Instead, the L.D.A. shows that the reduction of the moment capacity is more intense for a low heterogeneity degree.

Another important remark is related to the shape of the failure envelope. For a low heterogeneity degree κ_h = 0.4 and an S.D.A., the deduced shapes are quite similar and symmetric, which explains why a universal failure envelope is derivable. This fact is not observed for higher heterogeneity degrees, as shown in Fig. 7b, where the shapes are undoubtedly dissimilar. On the other hand, for a L.D.A., the non- symmetric form of the failure envelope is obvious due to the vertical load level effect combined with the slenderness ratio, independent of the heterogeneity degree level.

Cyclic pushover analysis

Results from a cyclic pushover L.D.A. are provided herein. A cyclic horizontal displacement at the elevated mass is applied and its magnitude is considered to gradually increase with the number of cycles. From the L.D.A., the moment and settlement responses with respect to the rotation angle are obtained, as shown in Fig. 8 and Fig. 9 for the vertical safety factors FS_v =5 and 2, respectively, and a slenderness ratio $\mathcal{H}/B$ = 2. For a relatively light structure (FS_v = 5), a strong softening behaviour is observed in the cyclic response, with reduction in peak moments being consistent with the monotonic response. The footing uplift at maximum rotation amplitude $|\vartheta_0|$ progressively increases with the number of cycles (see Fig. 8).

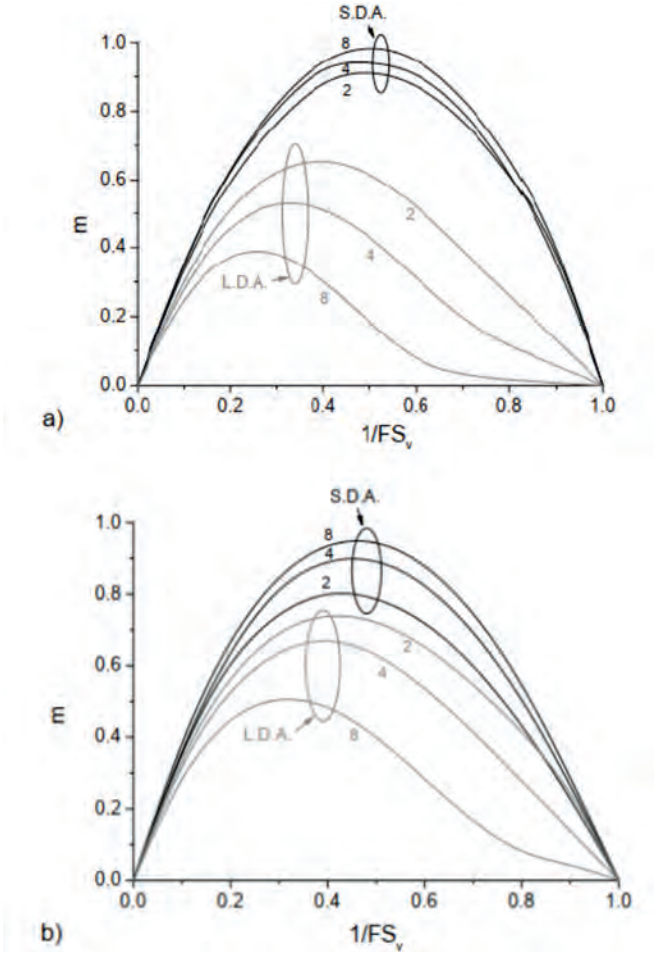

Fig. 7. Normalized moment capacity m with respect to the inverse vertical safety factor 1/FSv for different slenderness ratios $\mathcal{H}/B$ = (2,4,8), initial OCR = 4, heterogeneity degree κ_h = (0.4,2,4) with both (S.D.A.) small- and and (L.D.A.) large displacement analyses; a) κ_h = 0.4 and b) κ_h = 4

Rys. 7. Nośność znormalizowanego momentu m w odniesieniu do odwrotnego pionowego współczynnika bezpieczeństwa 1/ FSv dla różnych współczynników smukłości $\mathcal{H}/B$ = (2,4,8), początkowego OCR = 4, stopnia niejednorodności κ_h = (0,4,2,4) przy analizie zarówno (S.D.A.) małych i (L.D.A.) dużych przemieszczeń; a) κ_h = 0,4 i b) κ_h = 4

Conclusions

Two engineering problems of a surface strip footing under pure moment-vertical loading (M-V) and a thin structure-strip footing under moment-horizontal-vertical loading (M-H-V)

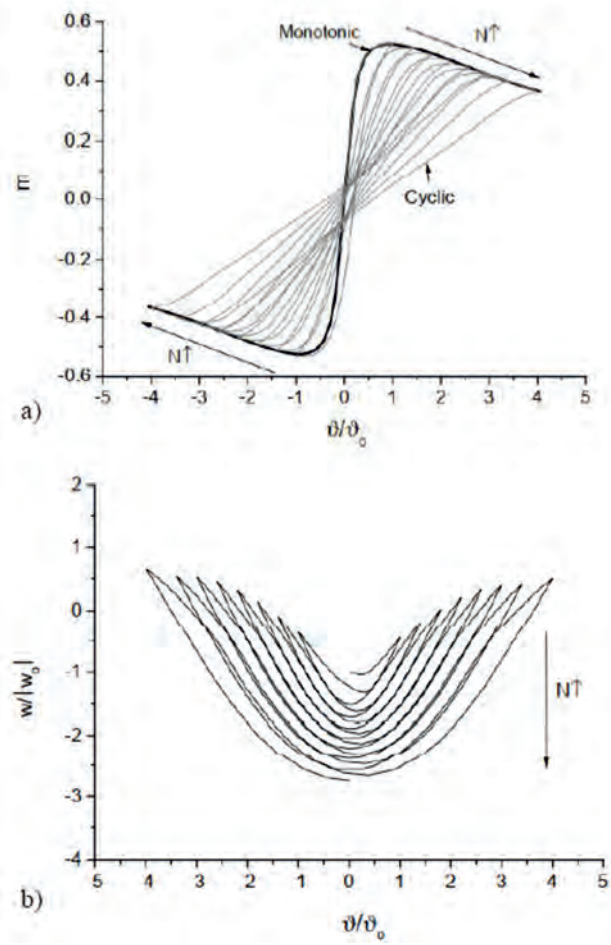

Fig. 8. (a) Moment and (b) normalized settlement with respect to the normalized rotation angle with ϑ_0 = 0.02rad for a vertical safety factor FS_v = 5, uniform OCR = 4, heterogeneity degree κ_h = 0.4, and initial settlement w_o = -3.7mm.

Rys. 8. (a) Moment i (b) znormalizowane osiadanie względem znormalizowanego kąta obrotu o ϑ_0 = 0,02rad dla pionowego współczynnika bezpieczeństwa FS_v = 5, jednolitego OCR = 4, stopnia niejednorodności κ_h = 0,4 oraz osiadania początkowego w_o = -3,7mm.

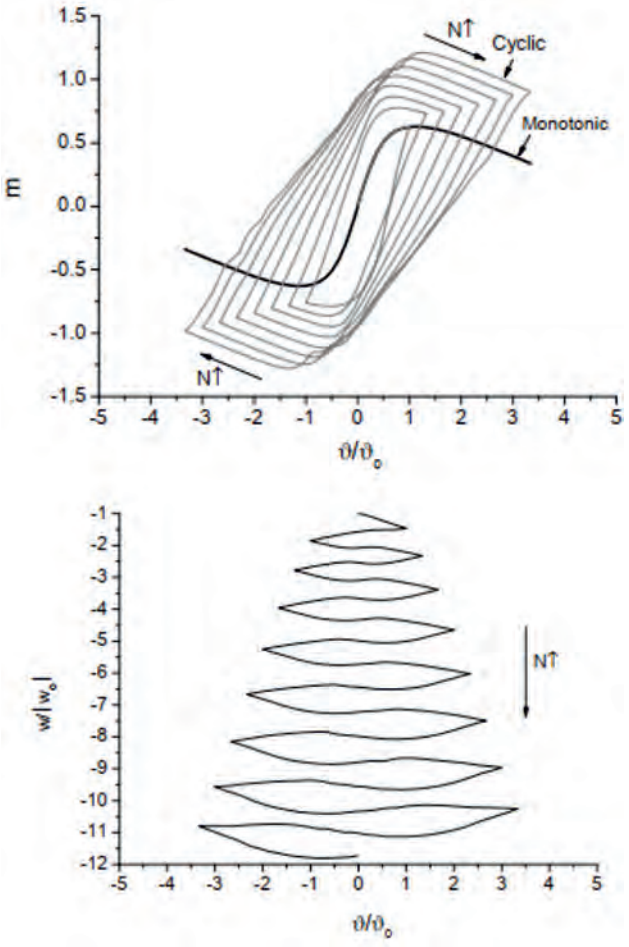

Fig. 9. Moment and normalized settlement with respect to the normalized rotation angle with ϑ_0 = 0.02rad for a vertical safety factor FS_v = 2, uniform OCR = 4, heterogeneity degree κ_h = 0.4, and initial settlement w_o = -10.7mm.

Rys. 9. Moment i znormalizowane osiadanie względem znormalizowanego kąta obrotu o ϑ_0 = 0,02rad dla pionowego współczynnika bezpieczeństwa FS_v = 2, jednorodnego OCR = 4, stopnia niejednorodności κ_h = 0,4 i osiadania początkowego w_o = -10,7mm.

resting on a heterogeneous clay (linearly increasing undrained shear strength) deposit subjected to a monotonic or cyclic load action were implemented in finite element analyses (ABAQUS). Two interface types were considered: (1) the fully-bonded interface and (2) the tensionless interface. To enable a realistic representation of the soil response under cyclic loading, an advanced constitutive soil model is adopted, which can capture pore-pressure and strength degradation effects. It was found that, for combined loading of shallow foundations, the bearing capacity factors are significantly higher when a fully-bonded interface is considered when compared to the tensionless interface case. For a pure moment-vertical load action, the shape of the failure envelope is highly affected by the interface properties. Since the main application of the current project is the onshore wind turbines and their associated foundation systems, the focus is placed on the assumption of the tensionless interface. For the thin structure-footing system under M-H-V loading, a dominant footing uplift mechanism is obtained for light structures and the opposite holds for heavily loaded structures, where a significant settlement accumulation occurs during cyclic loading. For a typical vertical safety factor (FSv < 5) anticipated in practice, a mixed mechanism is more frequently observed. In particular, even if footing uplift may be initially present, its magnitude is progressively reduced as the number of cycles increases due to material nonlinearities. Based on the analysis, the moment bearing capacity of the thin structure-footing system decreases as the slenderness ratio and/or the vertical safety factor increases, and the opposite mechanism is obtained as the heterogeneity degree increases. If a large deformation analysis (L.D.A.) is considered, the moment capacity non-symmetry decreases with the slenderness ratio, while the opposite holds for a small deformation analysis (S.D.A.), regardless of the heterogeneity degree. If the L.D.A. is activated, the reduction of the moment capacity is more significant for a low heterogeneity degree.

Acknowledgements

This work received funding from the EU's Research Fund for Coal and Steel under the projects "SUMAD – Sustainable Use of Mining Waste Dumps" Grant No. 847227.

References

[1] Andersen, K. 2015. *Cyclic soil parameters for offshore foundation design. In Frontiers in Offshore Geotechnics III,* pp. 5–82. CRC Press.

[2] Andersen, K. H., A. Kleven, and D. Heien. 1988. *Cyclic soil data for design of gravity structures.* Journal of Geotechnical Engineering 114 (5), 517–539.

[3] Butterfield, R., G. T. Houlsby, and G. Gottardi. 1997. Standardized sign conventions and notation for generally loaded foundations. Géotechnique 47 (5), 1051–1054.

[4] Dafalias, Y. F. 1986. *Bounding surface plasticity. I: Mathematical foundation and hypoplasticity.* Journal of Engineering Mechanics 112 (9), 966–987.

[5] Dafalias, Y. F. and L. R. Herrmann. 1986. *Bounding surface plasticity II. application to isotropic cohesive soils.* Journal of Engineering Mechanics 112 (12), 1263–1291.

[6] Gazetas, G., Anastasopoulos, I., Adamidis, O., Kontoroupi, T., 2013. *Nonlinear rocking stiffness of foundations.* Soil Dynamics and Earthquake Engineering 47, 83–91.

[7] Kaliakin, V. N. and Nieto-Leal, A. 2013. *Towards a Generalized Bounding Surface Model for Cohesive Soils.* In Fifth Biot Conference on Poromechanics.

[8] Masoudian, M. S., Zevgolis, I. E., Deliveris, A. V., Marshall, A. M., Heron, C. M., & Koukouzas, N. C. (2019a). *Stability and characterisation of spoil heaps in European surface lignite mines: a state-of-the-art review in light of new data.* Environmental Earth Sciences, 78(16), 1-18.

[9] Seidalinov, G. and M. Taiebat (2014). *Bounding surface SANICLAY plasticity model for cyclic clay behavior.* International Journal for Numerical and Analytical Methods in Geomechanics 38 (7), 702–724.

[10] Shi, Z., J. P. Hambleton, and G. Buscarnera. 2019. *Bounding surface elastoviscoplasticity: A general constitutive framework for rate-dependent geomaterials.* Journal of Engineering Mechanics 145 (3).

[11] Thian, S. and C. Lee. 2014. *Geotechnical characterisation of high plasticity offshore clay.* Journal of Scientific Research and Reports 3 (21), 2745–2756.

[12] Vulpe, C., Gourvenec, S., Power, M., 2014. *A generalised failure envelope for undrained capacity of circular shallow foundations under general loading.* Géotechnique Letters 4, 187–196.

[13] Zevgolis, I. E., Theocharis, A. I., Deliveris, A. V., Koukouzas, N. C., Roumpos, C., & Marshall, A. M. (2021). *Geotechnical characterization of fine-grained spoil material from surface coal mines.* Journal of Geotechnical and Geoenvironmental Engineering, 147(7), 04021050.

Heap of the Lubelski Węgiel Bogdanka coal mine, Poland